

Electronic Supplementary Information (ESI) for:

*Charge Carrier Transport and Trap Levels on Solution-
Processed Zn(II) Schiff Bases OLEDs*

José Carlos Germino,^{a} Rodrigo Araujo Mendes,^b Luís Gustavo Teixeira Alves Duarte,^c Fabiano Severo Rodembusch,^d Roberto L. A. Haiduke,^e and Luiz Pereira^{a*}*

*^ai3N – Institute of Nanostructures, Nanomodeling and Nanofabrication, Department of Physics,
University of Aveiro, Aveiro 3810-193, Portugal*

^bQuantum Theory Project, University of Florida, Gainesville, Florida 32611, USA

^cChemistry Institute, University of Campinas, Campinas – SP, Brazil

^dChemistry Institute, Federal University of Rio Grande do Sul, Porto Alegre – RS, Brazil

*^eSão Carlos Institute of Chemistry, University of São Paulo, Av. Trabalhador São-Carlense, 400,
CP 780, 13560-970 São Carlos, SP, Brazil*

***Corresponding author:** germino@ua.pt and luiz@ua.pt

1. TD-DFT triplet-state calculated energies

Zn-Salophen like complexes

Solvent specifications: solvent name = PFO, stoichiometry = C₁₃₀H₈₀, $\epsilon = 3$, refractive index = 1.725

Table S1. Zn(salophen).

State	Energy (eV)	Energy (nm)	Assignment*
1A''	2.2450	552.26	H -> L
1A'	2.5451	487.14	H -> L + 1
2A''	3.0673	404.21	H - 2 -> L
2A'	3.1386	395.03	H - 2 -> L + 1
3A''	3.2457	381.99	H - 6 -> L + 1
3A'	3.9537	313.59	H - 2 -> L + 1
4A'	4.2486	291.83	H - 3 -> L
4A''	4.3589	284.44	H - 2 -> L
5A''	4.4504	278.59	H - 3 -> L + 1
5A'	4.4853	276.42	H - 7 -> L + 1

*Largest coefficients

Table S2. Zn(sal-3,4-ben).

State	Energy (eV)	Energy (nm)	Assignment*
1 A	2.1776	569.37	H -> L
2 A	2.5229	491.43	H -> L + 1
3 A	2.9337	422.63	H - 2 -> L
4 A	3.0081	412.17	H - 5 -> L + 2
5 A	3.1091	398.78	H - 2 -> L + 1
6 A	3.1839	389.41	H - 1 -> L + 22
7 A	3.6227	342.24	H - 8 -> L + 2
8 A	3.8875	318.93	H - 2 -> L + 1
9 A	4.1524	298.59	H - 3 -> L
10A	4.2536	291.48	H - 3 -> L

*Largest coefficients

Table S3. Zn(BTS).

State	Energy (eV)	Energy (nm)	Assignment*
1 A	1.9434	637.97	H -> L
2 A	2.4624	503.50	H -> L + 1
3 A	2.6530	467.34	H - 2 -> L
4 A	2.9946	414.02	H - 2 -> L + 2
5 A	3.0479	406.79	H - 4 -> L + 1
6 A	3.1987	387.61	H - 9 -> L
7 A	3.8043	325.90	H -> L + 1
8 A	4.0320	307.50	H - 4 -> L
9 A	4.1363	299.75	H - 5 -> L
10A	4.2735	290.12	H - 5 -> L

*Largest coefficients

2. PFO and PFO:OXD-7 OLEDs optoelectronic properties

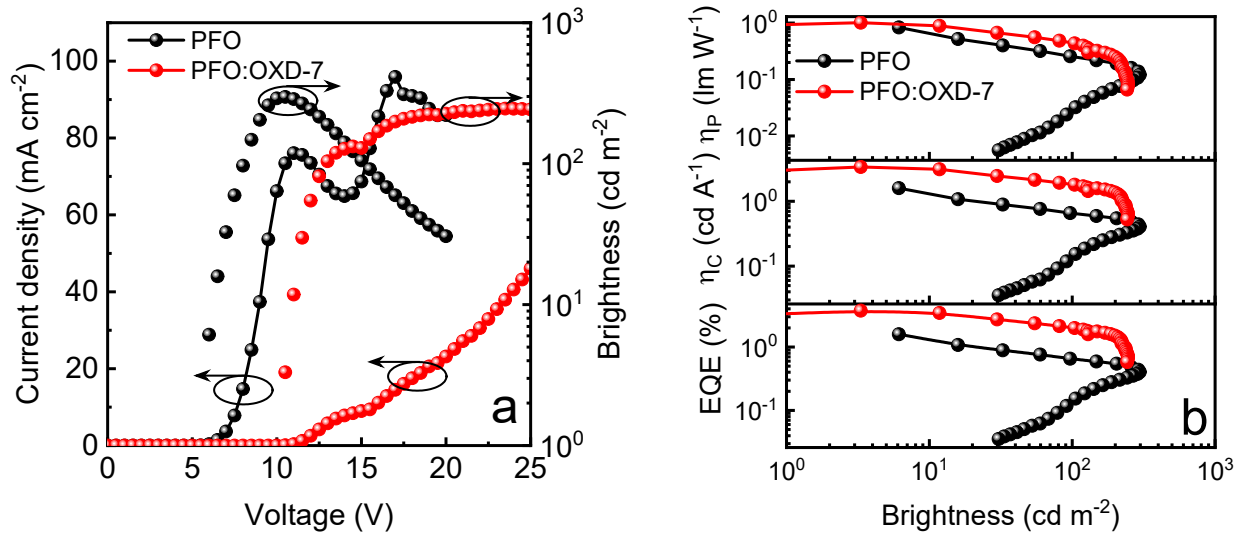


Figure S1. Current density and brightness *versus* voltage (a) and EQE, η_c and η_p *versus* brightness (b) curves of PFO (black curves) and PFO:OXD-7 (red curves) OLEDs.

3. PFO and PFO:OXD-7 with Zn(II) Schiff bases p- and n-type diodes

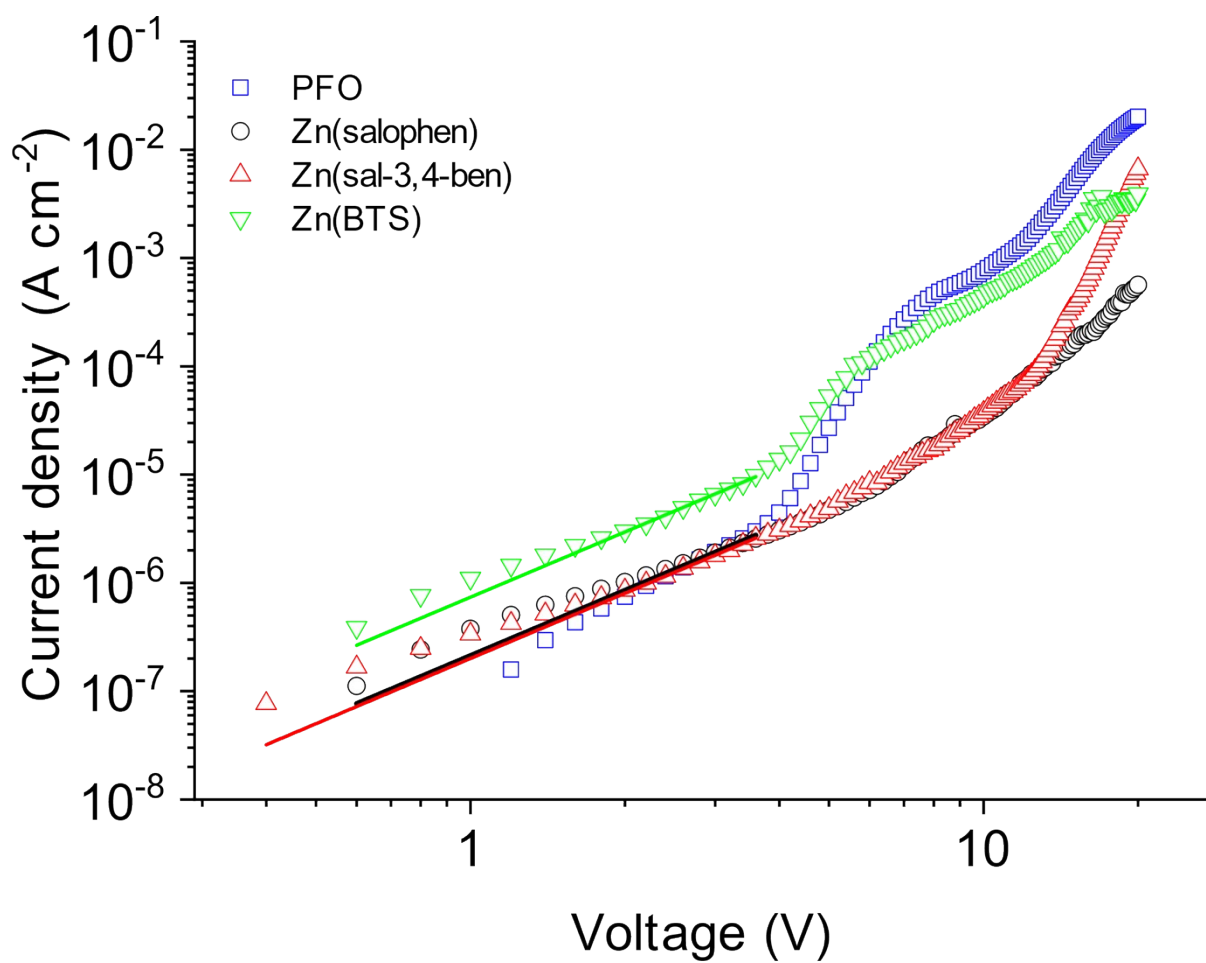


Figure S2. Current density Vs. voltage curves for p-type diodes of the Zn(II) Schiff base in PFO host active layers.

Table S4. Mott-Gurney (SCLC) fit parameters for p-type diodes of the Zn(II) Schiff base in PFO host active layers (a is the charge-carrier mobility; d is the active layer thickness; and e is the active layer dielectric constant).

Model	SCLC (User)			
Equation	$((9/8)*(8.85e-14*e)/(d^3))*a*(x^2)$			
Reduced Chi-Sqr	1.27074E-14	2.19736E-14	6.73203E-15	6.11525E-14
Adj. R-Square	0.9846	0.96235	0.98868	0.99259
		Value	Standard Error	
PFO	a	3.69852E-10	7.35527E-12	
	d	8E-6	0	
	e	3	0	
Zn(salophen)	a	3.6484E-10	9.66132E-12	
	d	8E-6	0	
	e	3	0	
Zn(sal-3,4-ben)	a	3.43587E-10	5.34751E-12	
	d	8E-6	0	
	e	3	0	
Zn(BTS)	a	1.2648E-9	1.61173E-11	
	d	8E-6	0	
	e	3	0	

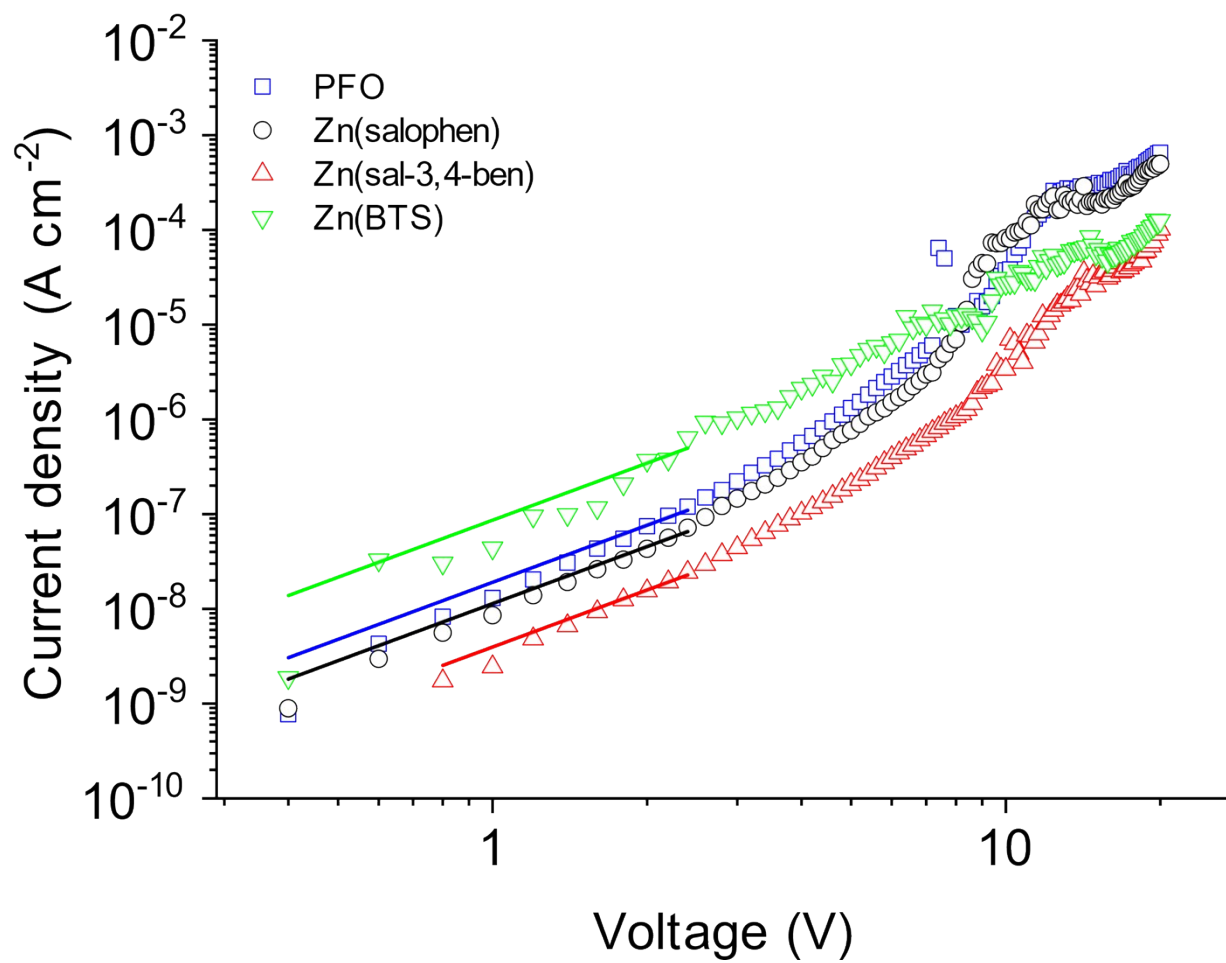


Figure S3. Current density Vs. voltage curves for n-type diodes of the Zn(II) Schiff base in PFO host active layers.

Table S5. Mott-Gurney (SCLC) fit parameters for n-type diodes of the Zn(II) Schiff base in PFO host active layers (a is the charge-carrier mobility; d is the active layer thickness; and e is the active layer dielectric constant).

Model		SCLC (User)			
Equation		$((9/8)*(8.85e-14*e)/(d^3))*a*(x^2)$			
Reduced Chi-Sqr		3.56172E-17	9.71868E-18	1.03748E-18	4.67599E-15
Adj. R-Square		0.97765	0.98209	0.98302	0.88327
		Value		Standard Error	
PFO	a	3.27025E-11	1.038E-12		
	d	8E-6	0		
	e	3	0		
Zn(salophen)	a	1.94745E-11	5.42213E-13		
	d	8E-6	0		
	e	3	0		
Zn(sal-3,4-ben)	a	6.78494E-12	1.77298E-13		
	d	8E-6	0		
	e	3	0		
Zn(BTS)	a	1.48044E-10	1.18933E-11		
	d	8E-6	0		
	e	3	0		

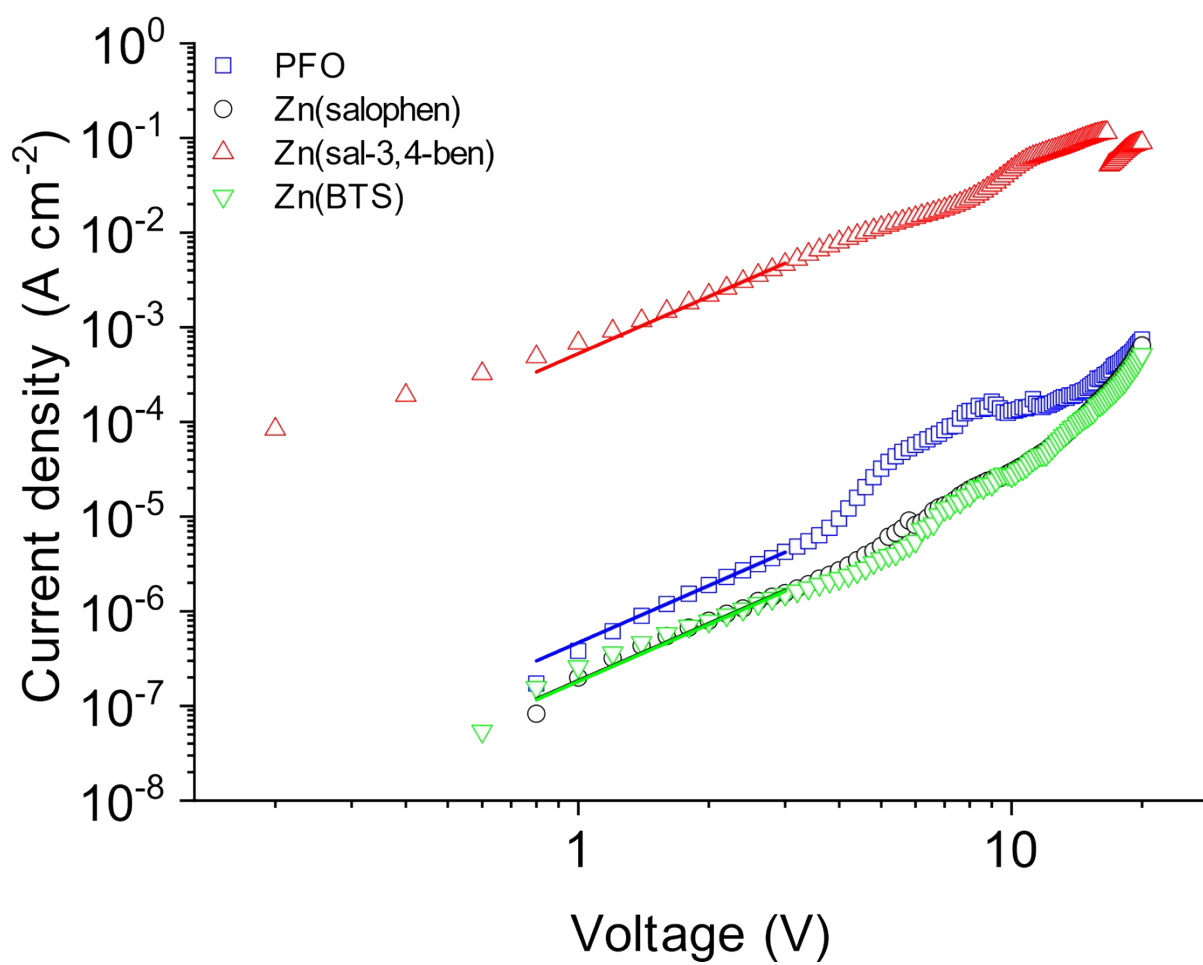


Figure S4. Current density Vs. voltage curves for p-type diodes of the Zn(II) Schiff base in PFO:OXD-7 host active layers.

Table S6. Mott-Gurney (SCLC) fit parameters for p-type diodes of the Zn(II) Schiff base in PFO:OXD-7 host active layers (a is the charge-carrier mobility; d is the active layer thickness; and e is the active layer dielectric constant).

Model	SCLC (User)			
Equation	$((9/8)*(8.85e-14*e)/(d^3))*a*(x^2)$			
Reduced Chi-Sqr	2.95E-15	3.50E-15	1.30E-08	7.24E-15
Adj. R-Square	0.99832	0.98513	0.99307	0.96266
		Value	Standard Error	
PFO:OXD-7	a	8.00E-10	5.52E-12	
	d	8.00E-06	0	
	e	3	0	
Zn(salophen)	a	3.17E-10	6.01E-12	
	d	8.00E-06	0	
	e	3	0	
Zn(sal-3,4-ben)	a	9.04E-07	1.16E-08	
	d	8.00E-06	0	
	e	3	0	
Zn(BTS)	a	3.11E-10	8.64E-12	
	d	8.00E-06	0	
	e	3	0	

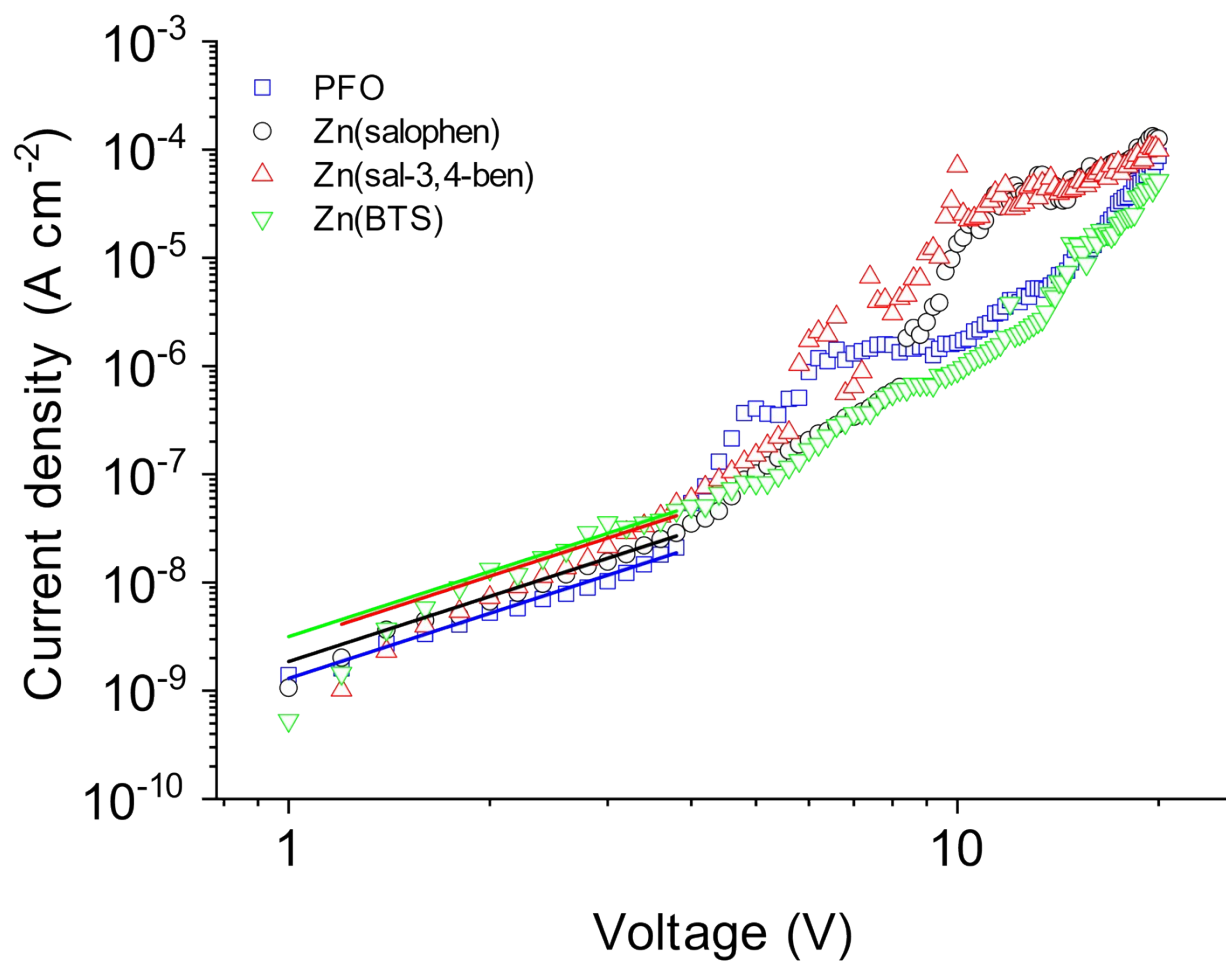


Figure S5. Current density Vs. voltage curves for n-type diodes of the Zn(II) Schiff base in PFO:OXD-7 host active layers.

Table S7. Mott-Gurney (SCLC) fit parameters for n-type diodes of the Zn(II) Schiff base in PFO:OXD-7 host active layers (a is the charge-carrier mobility; d is the active layer thickness; and e is the active layer dielectric constant).

Model	SCLC (User)			
Equation	$((9/8)*(8.85e-14*e)/(d^3))*a*(x^2)$			
Reduced Chi-Sqr	9.03201E-19	8.95647E-19	2.72156E-17	9.16925E-18
Adj. R-Square	0.97476	0.98813	0.89244	0.95941
		Value	Standard Error	
PFO:OXD-7	a	2.22745E-12	5.43121E-14	
	d	8E-6	0	
	e	3	0	
Zn(salophen)	a	3.19232E-12	5.40845E-14	
	d	8E-6	0	
	e	3	0	
Zn(sal-3,4-ben)	a	4.90716E-12	2.98301E-13	
	d	8E-6	0	
	e	3	0	
Zn(BTS)	a	5.42067E-12	1.7305E-13	
	d	8E-6	0	
	e	3	0	

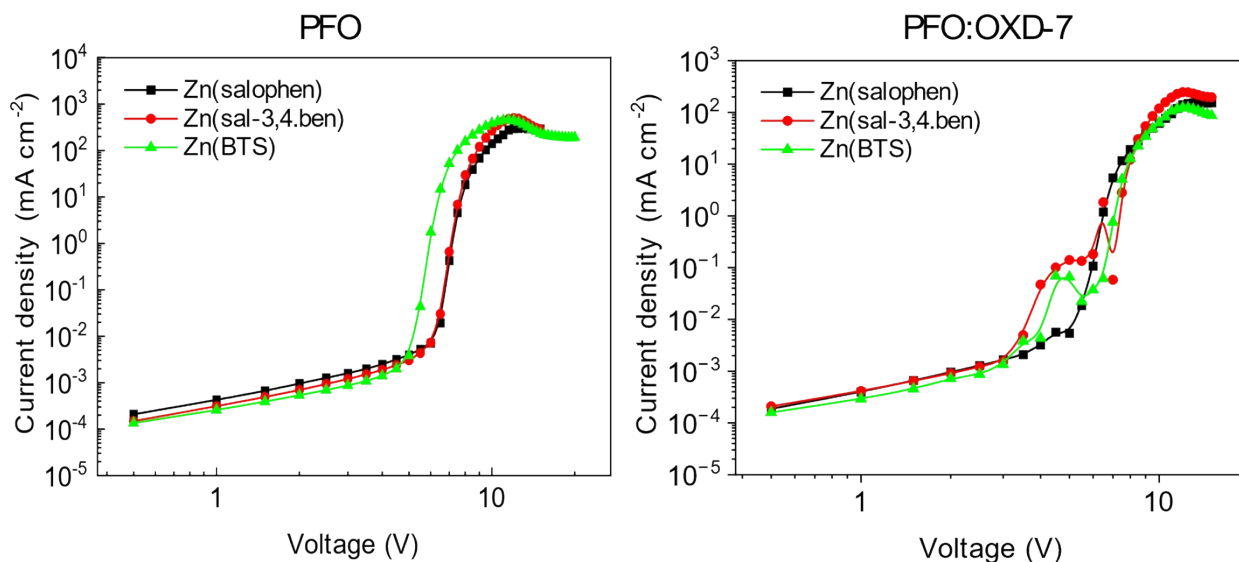


Figure S6. Log x Log plot of current density Vs. voltage curves for Zn(II) Schiff base-based OLEDs in PFO (right) and PFO:OXD-7 (left) host matrices.

3. Optical-electronic properties of PFO and PFO:OXD-7 with Zn(II) Schiff bases processed in hot conditions

Supplementary text 1

One of many challenges in using neat PFO as a host material is directly linked to the high crystallinity of its polymer chains.¹ In fact, the annealing process is well-known for enhancing the optoelectronic properties of the OLED.² This behavior is due to the better molecules, transition dipole moment orientation, and electronic density conformation of the materials inside the emissive layer.³ In this sense, we also fabricated a series of devices including a step of annealing after active layers deposition. The complete data-set for these devices are related in Fig. S6 to S9. However, in the case of the PFO polymer, the annealing process leads to phase separation among the materials that constitute the active layer, enhancing PFO crystallinity while simultaneously aggregating emissive dopants. In those cases, the PFO emission completely overlaps with the guest emission. Then, only the PFO electroemission band could be observed. To solve these problems involving phase segregation in PFO-based active matrices but in a processing alternative that results in a high-order of crystallinity, we also spin-coated the PFO and PFO:OXD-7 emissive layers when their solutions were close to the THF boiling point ($T = 55\text{ }^{\circ}\text{C}$; hot). The total density of the trap states of these devices was calculated in the same way as that of the room-temperature (cold) OLEDs previously presented (Fig. S9a and S9b). Finally, related to this attempt to optimize the solution-processing conditions of PFO and PFO:OXD-7 devices, the temperature parameter increases the N_T values in all cases, and clearly, the addition of Zn(II)Schiff bases, even at very low concentrations, can decrease the N_T values under normal (cold) processing conditions, which is directly linked to the better performance parameters than those of the control OLEDs (PFO and PFO:OXD-7).

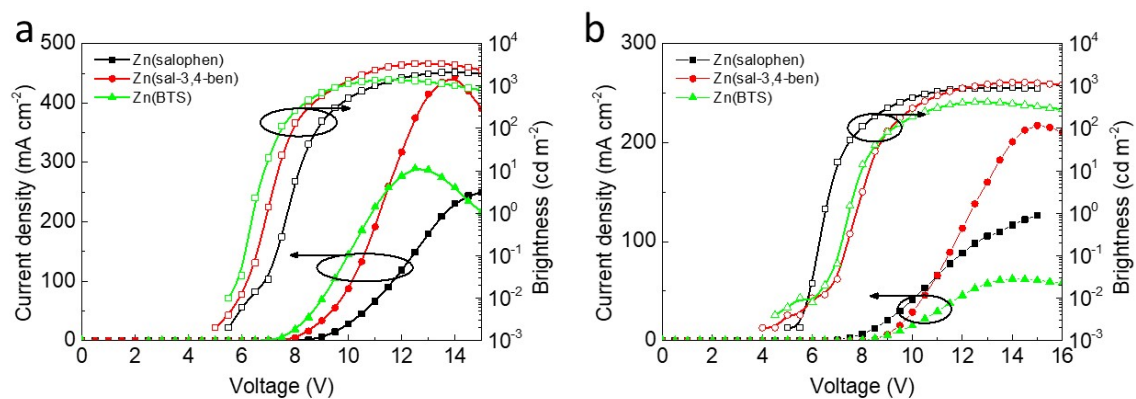


Figure S7. Current density (full symbols) and luminance (open symbols) versus voltage curves of the Zn(II) Schiff base OLEDs in PFO (a) and PFO:OXD-7 (b) host matrices processed under hot condition.

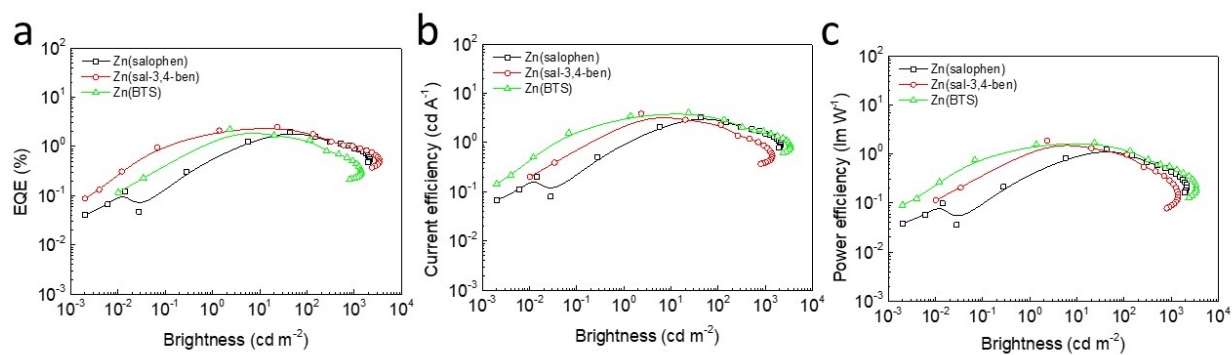


Figure S8. Diodes optical-electronic properties in terms of EQE, current efficiency and power efficiency of the Zn(II) Schiff base in PFO host matrix processed under hot condition.

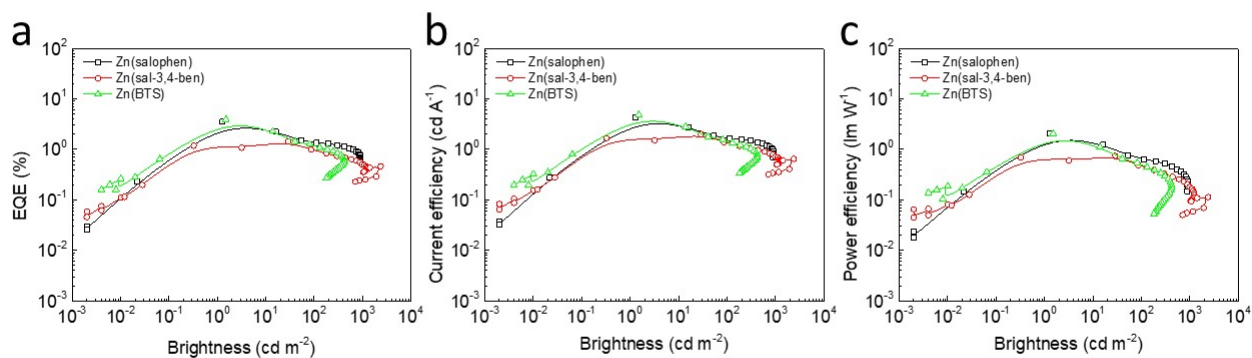


Figure S9. Diodes optical-electronic properties in terms of EQE, current efficiency and power efficiency of the Zn(II) Schiff base in PFO:OXD-7 host matrix processed under hot condition.

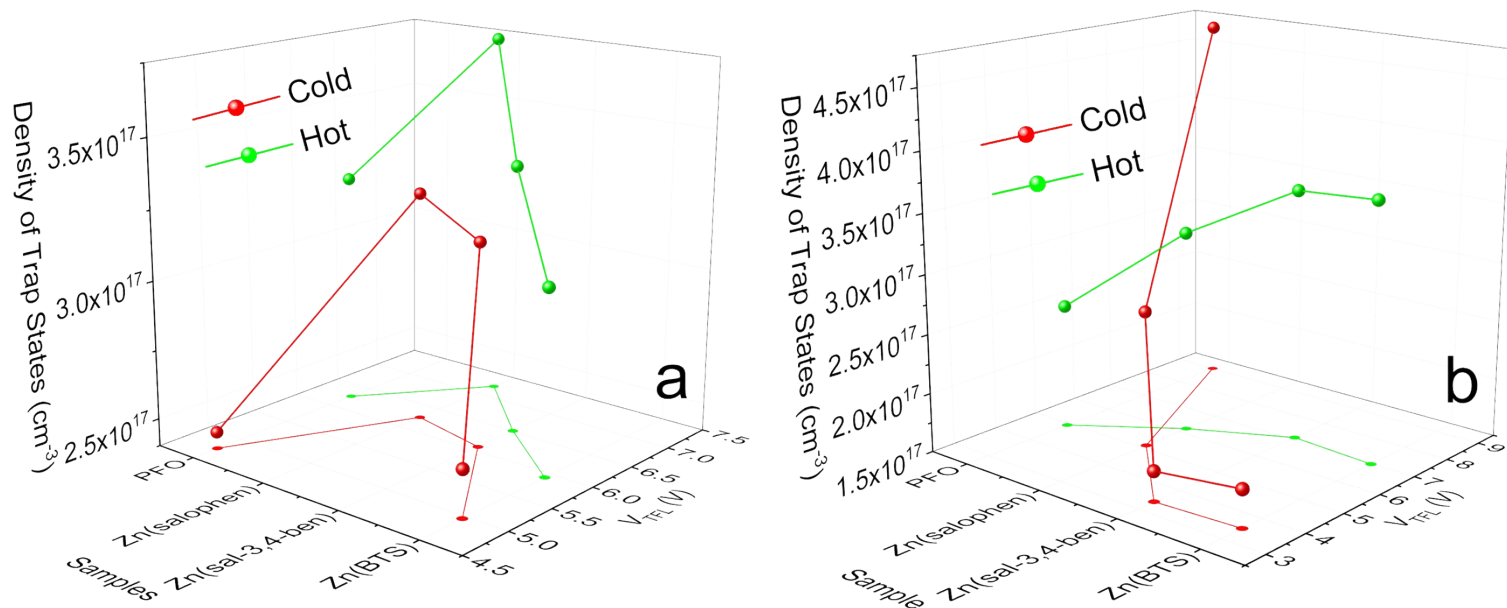


Figure S10. Density of trap state distributions of Zn(II) Schiff base diodes with PFO (a) and PFO:OXD-7 (b) as host matrices under cold (red curves) and hot (green curves) processability conditions.

References

- 1 M. N. Yu, H. Soleimaninejad, J. Y. Lin, Z. Y. Zuo, B. Liu, Y. F. Bo, L. B. Bai, Y. M. Han, T. A. Smith, M. Xu, X. P. Wu, D. E. Dunstan, R. D. Xia, L. H. Xie, D. D. C. Bradley and W. Huang, *Journal of Physical Chemistry Letters*, 2018, 9, 364–372.
- 2 C. Kant, A. Shukla, S. K. M. McGregor, S. C. Lo, E. B. Namdas and M. Katiyar, *Nat Commun*, DOI:10.1038/s41467-023-43014-7.
- 3 S. Wang, Z. Zhu, C. Shi, S. Li, Y. Liu, D. Zhang, Q. Wang, L. Zhao, W. Wang and X. Dong, *Spectrochim Acta A Mol Biomol Spectrosc*, DOI:10.1016/j.saa.2022.120933.